THE JOURNAL OF PHYSICAL CHEMISTRY B

Article

pubs.acs.org/JPCB

Immersion Depth of Surfactants at the Free Water Surface: A Computer Simulation and ITIM Analysis Study

Nóra Abrankó-Rideg,[†] Mária Darvas,[‡] George Horvai,[§,∥] and Pál Jedlovszky*[,†,§,⊥]

[†]Laboratory of Interfaces and Nanosize Systems, Institute of Chemistry, Eötvös Loránd University, Pázmány P. Stny 1/A, H-1117 Budapest, Hungary

[‡]SISSA, Department of Biological and Statistical Physics, 265 via Bonomea, I-34136 Trieste, Italy

[§]MTA-BME Research Group of Technical Analytical Chemistry, Szt. Gellért tér 4, H-1111 Budapest, Hungary

[∥]Department of Inorganic and Analytical Chemistry, Budapest University of Technology and Economics, Szt. Gellért tér 4, H-1111 Budapest, Hungary

[⊥]EKF Department of Chemistry, Leányka u. 6, H-3300 Eger, Hungary

S *Supporting Information*

ABSTRACT: The adsorption layer of five different surfactants, namely, pentanol, octanol, dodecanol, dodecyl trimethyl ammonium chloride, and sodium dodecyl sulfate, has been analyzed on the basis of molecular dynamics simulation results at two surface densities, namely, 1 and 4 μmol/m^2. The analyses have primarily focused on the question of how deeply, in terms of atomistic layers, the different surfactant molecules are immersed into the aqueous phase. The orientation and conformation of the surfactant molecules have also been analyzed. The obtained results reveal a clear difference between the immersion behavior of the alcoholic and ionic surfactants. Thus, alcoholic surfactants are found to be located right at the water surface, their apolar tails not being considerably immersed into the aqueous phase and the alcoholic headgroups being preferentially located in the surface layer of water. Ionic surfactants are immersed several layers deep into the aqueous phase, with headgroup atoms reaching the sixth−eighth and tail carbon atoms reaching the third−fourth subsurface layer in several cases. The observed difference is related, on the one hand, to the ability of the alcoholic surfactants of substituting surface water molecules in their lateral hydrogen bonding network at the water surface and that of their apolar tails for replacing dangling hydrogens and, on the other hand, to the energetic gain of the ionic headgroups if they are fully hydrated rather than being in contact with hydrocarbon tail groups.

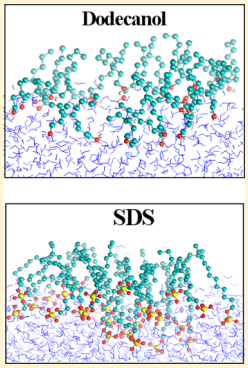

1. INTRODUCTION

Surfactants are textbook examples for surface active molecules, as they exhibit extremely strong adsorption at the surface of their aqueous solution. The water surface gets saturated at very low bulk phase concentration of surfactants and, correspondingly, the surface tension of such aqueous solutions decreases extremely rapidly with concentration at infinite dilution. This well-known behavior has numerous industrial applications, from extraction or emulsification to food technology and washing industry.

The molecular level explanation of this behavior is also well-known: surfactants, built up by chemically linked polar and apolar groups, can efficiently decrease the surface tension by turning their polar groups to the aqueous and apolar groups to the apolar phase at the interface. Very little is known, however, about the details of this kind of arrangement on the atomistic length scale. In particular, the question of how deeply can the apolar part of a surfactant molecule penetrate, in terms of molecular layers, into the aqueous phase has, to our knowledge, rarely been addressed. Instead, it is commonly assumed that there is no such immersion; in other words, the boundary between the polar and apolar parts of the adsorbed surfactant molecule coincides with the position of the interface itself. Although this assumption is certainly reasonable in a macroscopic sense, entropic considerations make it rather questionable on microscopic length scales.

The microscopic structure of adsorbed surfactant layers at the air−water as well as at water−organic liquid−liquid interfaces has been intensively studied both by various surface sensitive experimental methods[1−18] and by computer simulation[13,19−39] in the past two decades. However, despite the wealth of such investigations, studies that could verify or falsify the above assumption are almost nonexistent. Notable exceptions are the neutron reflection studies of Penfold and coworkers, who found that ∼30% of the alkyl chain of sodium dodecyl sulfate, tetradecyltrimethylammonium bromide, and other surfactants must be immersed in the aqueous phase at the air−water interface at concentrations close to the respective critical micellar concentration values.[1,2,9]

The lack of detailed studies on how deeply the apolar part of the adsorbed surfactant molecules penetrates into the aqueous phase, or, in other words, how far the intramolecular boundary

Received: February 19, 2013
Revised: June 18, 2013
Published: June 21, 2013

between the polar and apolar groups can be located from the position of the interface is certainly related to the fact that finding the accurate location of the interface itself is far from being a trivial task if the system is seen at atomistic resolution, as in the case of computer simulations. This problem originates from the fact that the surface of a macroscopically flat fluid phase is corrugated by capillary waves on the atomistic length scale. The problem of locating this corrugated, intrinsic surface of a fluid phase seen at atomistic resolution is closely related to the problem of determining the molecules that are located right at the surface of their phase, i.e., at the boundary with the opposite phase. This problem was neglected in computer simulation studies of interfacial systems for a long while, as the interfacial region was traditionally approximated by a flat slab parallel with the Gibbs dividing surface of the system. This approximation is analogous to the aforementioned assumption that neglects the surfactant immersion into the aqueous phase.

It has been realized in the past decade that in computer simulation studies it is important to determine the intrinsic interface and to identify the molecules that are located right at the interface with the opposite phase. Several different methods have been proposed to accomplish these tasks,[40−46] and it has also been demonstrated that the neglect of the effect of the capillary waves leads to large systematic error in the calculated interfacial properties,[43,47−50] and this error can even propagate to the calculated thermodynamic properties of the system.[51] Intrinsic surface-analyzing methods have also been applied to the adsorption layer of various surfactants at the water surface several times;[33−36,38] however, the problem of the immersion depth has not been addressed even by such studies yet.

Among the various intrinsic methods, the Identification of the Truly Interfacial Molecules (ITIM)[43] turned out to be an excellent compromise between computational cost and accuracy.[45] In an ITIM analysis a probe sphere is moved along a grid of test lines perpendicular to the macroscopic plane of the surface from the bulk opposite phase toward the interface. When the probe touches the first molecule of the phase of interest, its move along the given test line is stopped, and the touched molecule is marked being at the interface. Once all of test lines are taken into account, the full set of the interfacial molecules (i.e., molecules that are "seen" from the opposite phase) are determined.[43] Furthermore, by disregarding the interfacial layer of the molecules and repeating the entire procedure the molecules that constitute the second (third, etc.) molecular layer beneath the surface can also be identified.

We perform a detailed analysis of the immersion depth of various ionic and nonionic surfactant molecules into the aqueous phase at the free water surface on the basis of our previous computer simulation.[38] The consecutive layers of the aqueous phase are determined by means of the ITIM method.[43] This way the questions of (i) which subsurface layers of the aqueous phase also contain CH_2 groups or headgroup atoms of the surfactant molecules, (ii) how large of a part (in terms of CH_2 groups) of the apolar tail of the surfactant molecules can be immersed into the aqueous phase, and (iii) what is the composition of the subsequent subsurface molecular layers can be meaningfully addressed. The study is completed by an analysis of the conformation and orientation of the hydrocarbon chains.

To avoid the arbitrariness of the particular choice of the surfactant molecule and to study also the effect of the headgroup type as well as of the tail length on the calculated properties, we consider here five different surfactant molecules. Three of them, i.e., the anionic sodium dodecyl sulfate (SDS), the cationic dodecyl trimethyl ammonium chloride (DTAC), and the nonionic dodecanol (DA) have a 12-C-atoms-long apolar alkyl tail. The remaining two surfactants, i.e., octanol (OA) and pentanol (PA), also have an alcoholic polar group, such as DA; however, they have alkyl tails of different lengths. The structure of these surfactant molecules is shown in Figure 1. To study also the effect of the degree of saturation of the surface, we consider here two surface densities of the surfactants, namely, 1 μmol/m^2, when the surface is far from saturation, and 4 μmol/m^2, corresponding to a nearly saturated water surface.

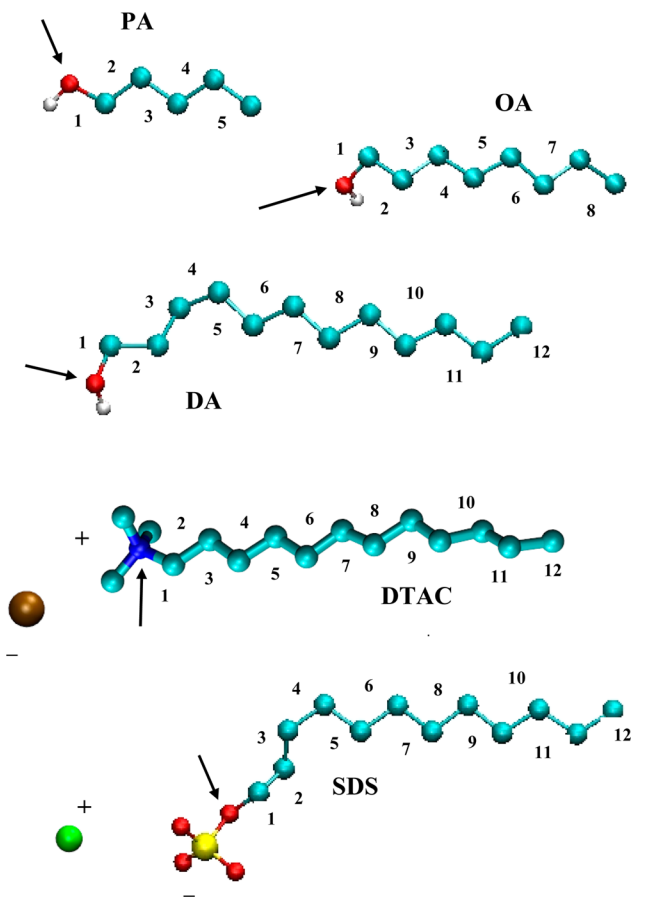

Figure 1. Structure of the five surfactants considered in this study. C, O, H, N, S, Na, and Cl atoms are shown by light-blue, red, white, dark blue, yellow, green, and brown colors, respectively. Hydrogens bound to a carbon atom are omitted for clarity. The numbering scheme of the C atoms used in the analyses is also indicated. The first atom of the headgroups, chemically bound to the C1 carbon atom of the tail, is marked by an arrow for all surfactants.

The paper is organized as follows. In Section 2, details of the simulations and ITIM analyses performed are given, and the way of defining the subsequent molecular layers of the aqueous phase is also described. In Section 3, the obtained results are discussed in detail. Finally, in Section 4, the main conclusions of this study are summarized.

2. COMPUTATIONAL DETAILS

2.1. Computer Simulations. The computer simulations on which the present study is based have already been described in

dx.doi.org/10.1021/jp401749r | J. Phys. Chem. B 2013, 117, 8733−8746

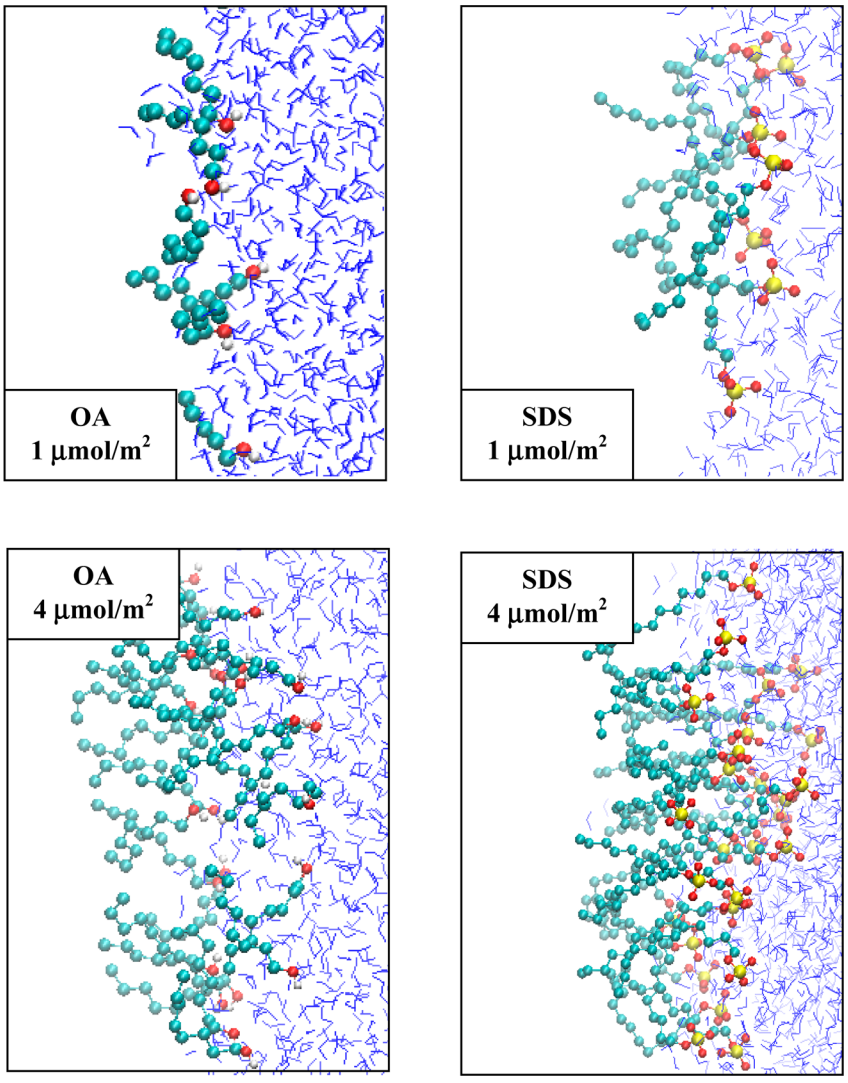

Figure 2. Instantaneous equilibrium snapshots (side view) of the surface region of the aqueous phase containing OA (left panels) and SDS (right panels) molecules adsorbed at the water surface at the surface densities of 1 μmol/m^2 (top panels) and 4 μmol/m^2 (bottom panels). Water molecules are shown by blue sticks; the O, C, and S atoms of the surfactants are indicated by red, light-blue, and yellow spheres, respectively. H atoms are omitted from the snapshots for clarity.

detail in our previous publication;[38] therefore, they are only briefly recalled here. Molecular dynamics simulations of the adsorption layer of five different surfactants, namely, PA, OA, DA, DTAC, and SDS, at the free water surface were performed on the canonical (N,V,T) ensemble at two different surface densities, namely, at 1 and 4 μmol/m^2. These surface densities correspond to unsaturated and saturated adsorption layers, respectively. The X, Y, and Z edges of the rectangular basic simulation box were 250.0, 31.41, and 31.41 Å long, respectively, with X being the axis perpendicular to the macroscopic plane of the interface. The basic box contained 1598 water molecules and 12 or 48 surfactants, depending on the surface density. (In the case of the ionic surfactants, the corresponding counterions were also contained by the basic box.) The temperature of the systems was 298 K. Standard periodic boundary conditions were applied.

The surfactants and counterions were described by the GROMOS96 force field[52,53] using the charge distribution proposed by Schweighofer and Benjamin for the headgroup of the dodecyl trimethyl ammonium (DTA) ion.[23] All bond lengths were kept fixed in the simulations by means of the LINCS algorithm,[54] while bond-angle bending and torsional rotation were included in the model. Torsional rotations were described by the Ryckaert−Bellemans potential function.[55] The CH_2 and CH_3 groups were treated as united atoms. Nonbonded interaction parameters of the potential models used are summarized in our previous publication,[38] whereas intramolecular parameters are listed in Tables S1 and S2 in the Supporting Information. Water molecules were described by the rigid, three-site SPC model;[56] their geometry was kept unchanged using the SETTLE algorithm.[57] All interactions were truncated to zero beyond the group-based cutoff distance of 15.0 Å; the long-range part of the electrostatic interaction was accounted for by means of the Particle Mesh Ewald (PME) method.[58]

The simulations were performed by the GROMACS 3.3.2 program package.[59] The temperature of the systems was controlled using the weak coupling algorithm of Berendsen et al.[60] The equations of motion were integrated in time steps of 1 fs. The simulations covered a 10 ns long trajectory, from which the first 5 ns were discarded. From the last 5 ns of the simulation runs, 1000 sample configurations, separated by 5 ps

dx.doi.org/10.1021/jp401749r | J. Phys. Chem. B 2013, 117, 8733−8746

long trajectories each, were used for detailed analyses. Equilibrium snapshots of the surface region of the 1 and 4 μmol/m^2 OA and SDS systems are shown in Figure 2, as taken out from the simulations.

2.2. Layer Definition and ITIM Analysis. When the immersion depth of the adsorbed surfactant molecules into the aqueous phase is investigated, the exact definition of the subsequent layers beneath the surface of the aqueous phase is of key importance. Clearly, the surfactant tails are expected to form a separate apolar region above the water surface. Thus, such tail carbon atoms (as parts of CH_2 or CH_3 groups) should not be regarded as part of the aqueous phase. One of the aims of the present study is to investigate if these hydrocarbon tails are, to a certain extent, immersed in water. This task can only be done by regarding the immersed tail carbon atoms as part of the aqueous phase. Therefore, a clear distinction has to be made between the carbon atoms that form the apolar layer above the water surface and the ones that are immersed into water. Taking this into account, we have defined the apolar layer to consist of all C atoms that have no water molecules as contact neighbors. These C atoms have been disregarded in the ITIM analysis. Tail C atoms having at least one contact water neighbor have been considered as part of the "aqueous" phase. It should be noted that although this definition can guarantee that no immersed tail C atom is missed from the aqueous phase, it has the certain drawback that C atoms that are above but in contact with water are still counted as part of the aqueous phase. In other words, the consequence of this treatment is that the first layer of the above-defined "aqueous phase" could include a substantial number of C atoms of surfactants that are laying on rather than immersed into the water phase. Although this artifact, which has to be kept in mind when interpreting the results of the present analyses, somewhat obscures the meaning of the "first layer of the aqueous phase", it cannot affect more than the very first atomistic layer of the aqueous phase, and hence the error introduced by this treatment into the analyses cannot exceed ±1 molecular layer.

To define the contact tail carbon−water pairs, we have calculated the radial distribution functions $g(r)$ between the first five tail carbons (see Figure 1) and water oxygen atoms in all systems simulated. The resulting functions are shown in Figure 3, as calculated in the 1 μmol/m^2 PA and SDS systems. Similar functions have been obtained in the other systems as well (data not shown). As is seen, the $g(r)$ function corresponding to the first, i.e., C1 carbon atom, exhibits a clear minimum at 4.5 Å. Tail carbon atoms having a water oxygen neighbor closer than this distance are thus regarded to have a contact water neighbor, and hence as being part of the aqueous phase. The tail C2−water O $g(r)$'s typically exhibit a shoulder at this critical distance, while this shoulder is gradually disappearing as going farther along the hydrocarbon tail of the surfactants. Nevertheless, even the C5 tail carbon atoms have contact water neighbors in several cases, indicating that at least some of the surfactant molecules are either laying on the water surface or deeply immersed into the aqueous phase. This point is addressed in detail in the following section. (Penetration of the apolar layer by some water molecules might also explain this observation, but this has been found to be a rare event.)

Another important point in the definition of the layers beneath the water surface is the question of whether individual atoms or larger atomic groups (e.g., the entire headgroup) of the surfactant molecules should be regarded as units that can

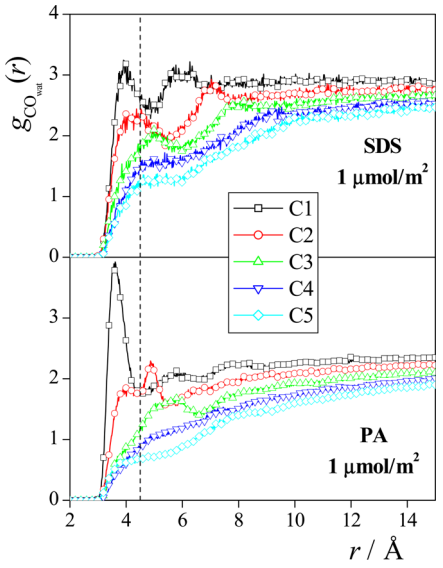

Figure 3. Radial distribution function of the water oxygen and C1 (black squares), C2 (red circles), C3 (green up triangles), C4 (dark-blue down triangles), and C5 (light-blue diamonds) carbon atoms of the hydrocarbon tail of the SDS (top panel) and PA (bottom panel) surfactant molecules at the surface density of 1 μmol/m^2. The numbering scheme of the tail carbon atoms is shown in Figure 1. The dashed vertical line at 4.5 Å shows the distance within which a water oxygen is regarded to be in contact with the tail carbon atom.

belong to a certain subsurface layer. Because the ITIM analysis, just like any intrinsic surface analyzing method,[45] contains a parameter of arbitrary choice, namely, the radius R_p of the sphere that probes the surface,[43] and in any reasonable choice R_p should be comparable to the size of the particles forming the surface layer,[43,45] in cases of mixed systems, ITIM can provide more accurate results if the different particles are of roughly the same size (and hence the probe sphere can also be in this size range). Therefore, here we regarded all of the O, S, N and C atoms of the surfactants as independent units in the ITIM analysis; and their sizes have been described by their Lennard-Jones radii. Since hydrogen atoms have either been regarded as part of the CH_2 or CH_3 groups represented as united atoms (which are often referred to here simply as "C atoms") or have not corresponded to Lennard-Jones interaction (as in the case of the water and alcoholic hydrogens), all H atoms have been disregarded in the present ITIM analyses.

In accordance with our previous findings,[43,45] a probe sphere of the radius of R_p = 1.25 Å and a 60 × 60 square-like grid of test lines have been used in the ITIM analyses. Depending on the system, three to eight subsequent subsurface layers have been determined in every case.

3. RESULTS AND DISCUSSION

3.1. Density Profiles. The number density profiles of the water O atoms, headgroup central atoms (i.e., O, N and S for the alcoholic surfactants, DTAC and SDS, respectively), tail C atoms, and, in the case of the ionic surfactants, also that of the Cl^- and Na^+ counterions, are shown in Figure 4. In the case of the 4 μmol/m^2 DTAC system, for which experimental data is available, the width of the tail carbon profile at half-maximum, σ_c, and the distance of the peaks of the Gaussian functions fitted to the N and tail C atom distributions, δ_{ch}, resulting in 10.0 and 5.9 Å, respectively, agree well with the data obtained from neutron reflectivity measurements of 10.9[2] and 6.0 Å,[9]

dx.doi.org/10.1021/jp401749r | J. Phys. Chem. B 2013, 117, 8733−8746

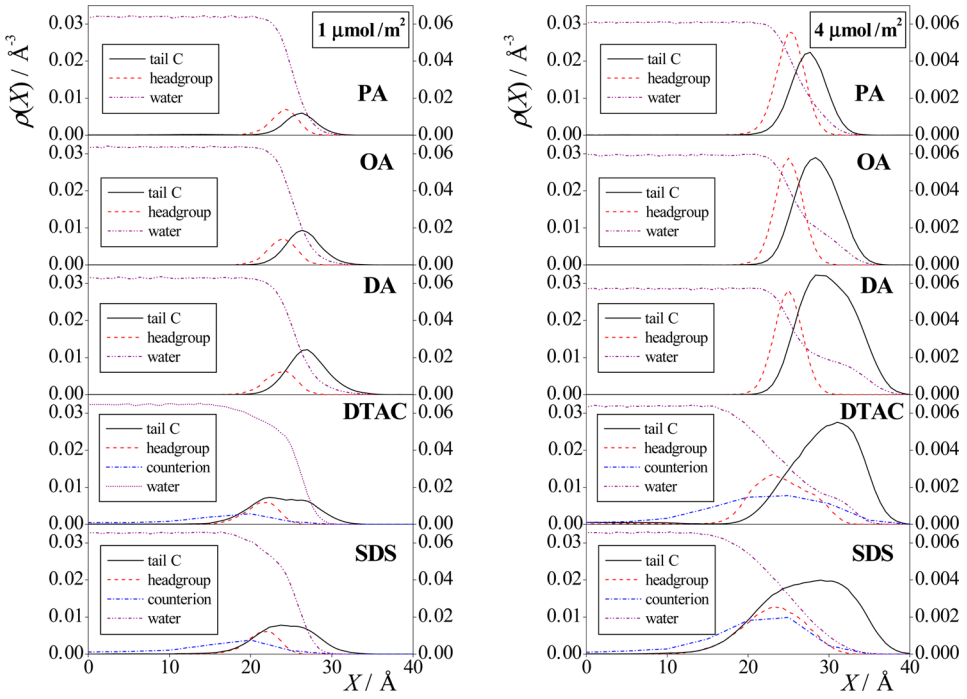

Figure 4. Number density profiles of the surfactant tail C atoms (black solid lines), headgroup central atoms (i.e., O for alcohols, N for DTAC, S for SDS, red dashed lines), counterions (blue dash-dotted lines), and water O atoms (purple dash-dot-dotted lines) along the surface normal axis X, as calculated in the systems containing PA (top panels), OA (second panels), DA (third panels), DTAC (fourth panels), and SDS (bottom panels) at the surface concentrations of 1 μmol/m^2 (left) and 4 μmol/m^2 (right). The scales at the left refer to the water O atom and hydrocarbon chain C atom, while those at the right refer to the headgroup central atom and counterion profiles. All of the profiles shown are symmetrized over the two liquid surfaces present in the basic simulation box.

respectively (the former value being corrected for the capillary wave contribution[20]). The obtained profiles, also being in sufficient agreement with results of previous simulations using different potential models,[20,37] indicate a much larger overlap of the water molecules and surfactant headgroups for the ionic than for the alcoholic surfactants. This finding suggests that ionic surfactants might immerse more deeply into the aqueous phase than the nonionic ones. However, nonintrinsic density profiles averaged over the entire cross-section of the simulation box do not separate the effect of surfactant immersion from that of the capillary waves. Thus, drawing such a conclusion solely from the density profiles is based on the (hidden) assumption that the surfactant headgroup type does not affect the roughness of the surface of the aqueous phase. To eliminate such hidden assumptions and thoroughly address the question of immersion, intrinsic surface analysis has to be performed. Results of this analysis are discussed in detail in a subsequent subsection.

3.2. Orientation and Conformation of the Surfactants.

Before investigating the immersion of the different surfactants in the aqueous phase, we briefly analyze their conformation and orientation in the different systems. Figure 5 shows the distribution of the cosine of angle ϑ, formed by the vector $\underline{l}$ pointing along the hydrocarbon tail, from the chain terminal CH_3 group to the first headgroup atom (i.e., alcoholic O, N, and C−O−S bonded O for the alcohols, DTAC and SDS, respectively) and the vector $\underline{X}$ being perpendicular to the macroscopic water surface and pointing from the aqueous to the vapor phase, as obtained in all ten systems simulated. As is seen, in the saturated systems the surfactant tails prefer to align perpendicular to the macroscopic water surface, and this preference is somewhat stronger for the ionic than for the

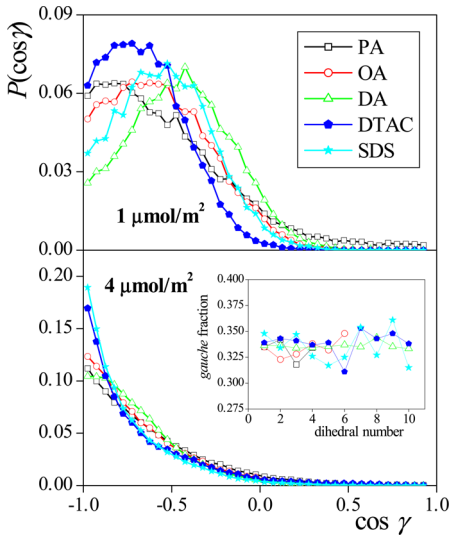

Figure 5. Distribution of the cosine of the angle ϑ formed by the vector pointing along the hydrocarbon tail (i.e., from its terminal CH_3 group to the first headgroup atom) and the surface normal vector, $\underline{X}$, pointing from the aqueous to the vapor phase in the systems containing PA (black squares), OA (red circles), DA (green triangles), DTAC (dark-blue pentagons), and SDS (light-blue stars) surfactants at the surface densities of 1 μmol/m^2 (top panel) and 4 μmol/m^2 (bottom panel). Open and filled symbols correspond to nonionic and ionic surfactants, respectively. The inset shows the fraction of the gauche aligned dihedrals along the hydrocarbon chain in the 4 μmol/m^2 systems.

alcoholic surfactants. In the systems of 1 μmol/m^2 surface density, where the surfactants can easily occupy rather large

dx.doi.org/10.1021/jp401749r | J. Phys. Chem. B 2013, 117, 8733−8746

portions of the water surface, this perpendicular orientational preference is no longer valid; the molecules prefer various tilted orientations relative to the water surface. The preference for such orientations reflects the conformational entropy of the hydrocarbon chains as well as their energetic gain if they are in contact with the water surface.

The length distribution of the vector l, pointing along the surfactant tail, is shown in Figure 6 for the ten systems

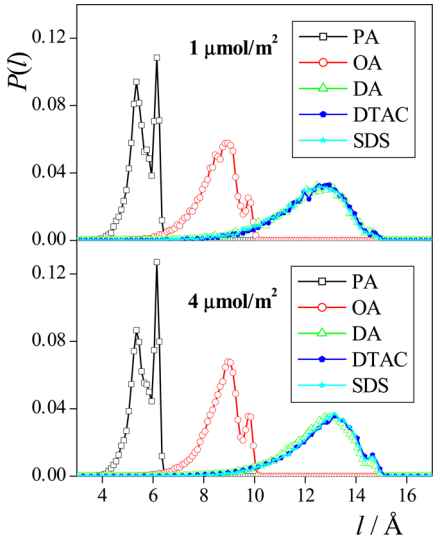

Figure 6. Distribution of the length l of the hydrocarbon tail (i.e., the distance of its terminal CH_3 group and the first headgroup atom) in the systems containing PA (black squares), OA (red circles), DA (green triangles), DTAC (dark-blue pentagons), and SDS (light-blue stars) surfactants at the surface densities of 1 μmol/m^2 (top panel) and 4 μmol/m^2 (bottom panel). Open and filled symbols correspond to nonionic and ionic surfactants, respectively.

simulated. These distributions indicate that surfactants prefer rather elongated conformations at the water surface. All distributions show a sharp peak at its large distance end and a rather broad peak, extending to small distances at a ~1.5 Å smaller l value. These peaks correspond to the all-trans and the one-gauche conformations, respectively, while conformations containing more than one gauche-aligned dihedrals give contribution to the long tail of the latter peak, extending to small l values. The fact that although all of the dihedrals prefer the trans alignment the probability of the gauche alignment is far from being negligible in every case (see the inset of Figure 5) leads to decreasing probability of the all-trans conformation with increasing chain length. (In the case of the dodecyl surfactants the height of the all-trans peak is so small that it almost turned to a shoulder.)

It is seen that the $P(l)$ distributions of the three dodecyl tail surfactants are almost identical to each other at both surface densities, indicating that tail conformation does not depend on the headgroup type. It is also clear that the $P(l)$ distribution obtained at 1 μmol/m^2 is always somewhat broader than that at the saturated surface, indicating again that at unsaturated surfaces the surfactant tails have larger conformational freedom.

It should finally be noted that the average length of the projection of the hydrocarbon chain to the surface normal axis, $\langle l_X \rangle$, resulting in 9.6 Å for the 4 μmol/m^2 DTAC system, compares well with the experimental value of 8.9 Å, obtained by neutron reflection measurement assuming that $\langle l_X^2 \rangle = \langle l^2 \rangle \langle \cos^2 \vartheta \rangle$.[9]

Besides the orientation of the hydrocarbon tail, we have also investigated how straight the headgroup of the surfactants points into the bulk aqueous phase. For this purpose, we have calculated the cosine distribution of the angle γ, formed by the chemical bond connecting the apolar and polar parts of the surfactant (i.e., pointing from the C1 tail to the first headgroup atom) and the macroscopic surface normal vector $\underline{X}$. The resulting distributions, shown in Figure 7, indicate that the

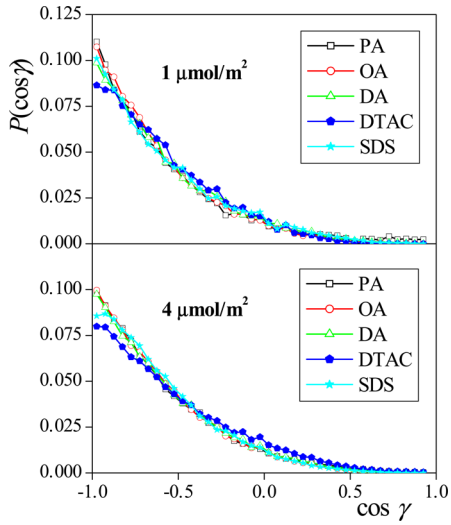

Figure 7. Distribution of the cosine of the angle γ formed by the vector pointing from the C1 carbon atom of the hydrocarbon tail to the first headgroup atom to which it is chemically bound and the surface normal vector, $\underline{X}$, pointing from the aqueous to the vapor phase in the systems containing PA (black squares), OA (red circles), DA (green triangles), DTAC (dark-blue pentagons), and SDS (light-blue stars) surfactants at the surface densities of 1 μmol/m^2 (top panel) and 4 μmol/m^2 (bottom panel). Open and filled symbols correspond to nonionic and ionic surfactants, respectively. The C1 tail carbon and first headgroup atoms are shown in Figure 1 for all surfactants.

surfactant molecules prefer to point straight into the bulk aqueous phase with their headgroup in every case, even at unsaturated surfaces, and this preference is largely independent of the surface density.

All of these results suggest that the surfactant headgroups are probably immersed in the aqueous phase into the depth of several molecular layers, and this immersion is likely to be somewhat deeper at large surface densities, when the surfactants preferentially align perpendicular to the macroscopic surface plane and their conformation is also more elongated than in unsaturated systems. This point is addressed in detail in the following subsection.

3.3. Immersion Depth of the Surfactants. To analyze the immersion depth of the various surfactant molecules, first we have calculated the hydration number, N_{hyd}, (i.e., the number of contact water neighbors, see Section 2.2 and Figure 3) of the first five C atoms of the hydrocarbon tails in the ten systems simulated. The average values of N_{hyd} are shown in Figure 8, whereas the distribution of the hydration number of these C atoms of the three dodecyl surfactants is shown in Figures 9 and 10 for the surface densities of 1 and 4 μmol/m^2, respectively. Distributions obtained for PA and OA (not

dx.doi.org/10.1021/jp401749r | J. Phys. Chem. B 2013, 117, 8733−8746

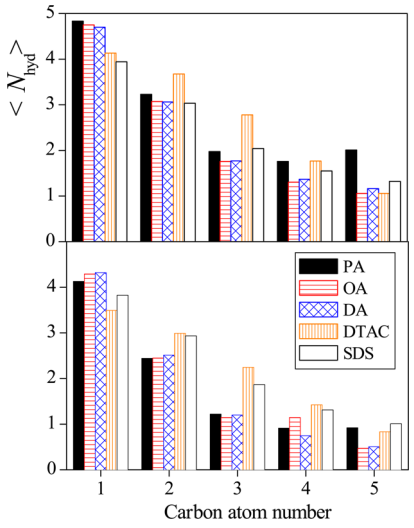

Figure 8. Average hydration number of the first five carbon atoms of the hydrocarbon tail of PA (black, filled columns), OA (red, horizontally striped columns), DA (blue, squared columns), DTAC (orange, vertically striped columns), and SDS (empty columns) in the systems of 1 μmol/m^2 (top) and 4 μmol/m^2 (bottom) surface densities. Tail carbon atoms are numbered from the headgroup toward the terminal methyl group (see Figure 1).

shown) turned out to be, in general, rather similar to those of the third alcoholic surfactant, DA.

As is seen, the observed hydration numbers are usually considerably larger, by about 1 unit, at the unsaturated than at the saturated surface, in accordance with our previous finding that surfactants prefer tilted alignments (i.e., more contact with water) at 1 μmol/m^2 and perpendicular alignment relative to the surface at 4 μmol/m^2. (See Figure 5.) Furthermore, the first C atom of the hydrocarbon tails is always well-hydrated, having, on average, four to five water neighbors in the unsaturated systems and around four water neighbors in the saturated systems. This finding is in a clear accordance with the observed tail carbon−water oxygen radial distribution functions. (See Figure 3.) The distribution of this hydration number is rather broad, always extending to eight to nine contact water neighbors and having its maximum at three−six contact water neighbors. (See Figures 9 and 10.) Upon going farther from the headgroup, the hydration number gradually decreases. The distribution of N_{hyd} becomes monotonous at the third tail C atom for the alcoholic and at the fourth tail atom for the ionic surfactants. In other words, from these C atoms on, the tail C atoms have preferentially no contact water neighbors. Nevertheless, even for the fifth tail carbon atom the mean hydration number is ∼1 in all systems simulated, and C5 atoms having

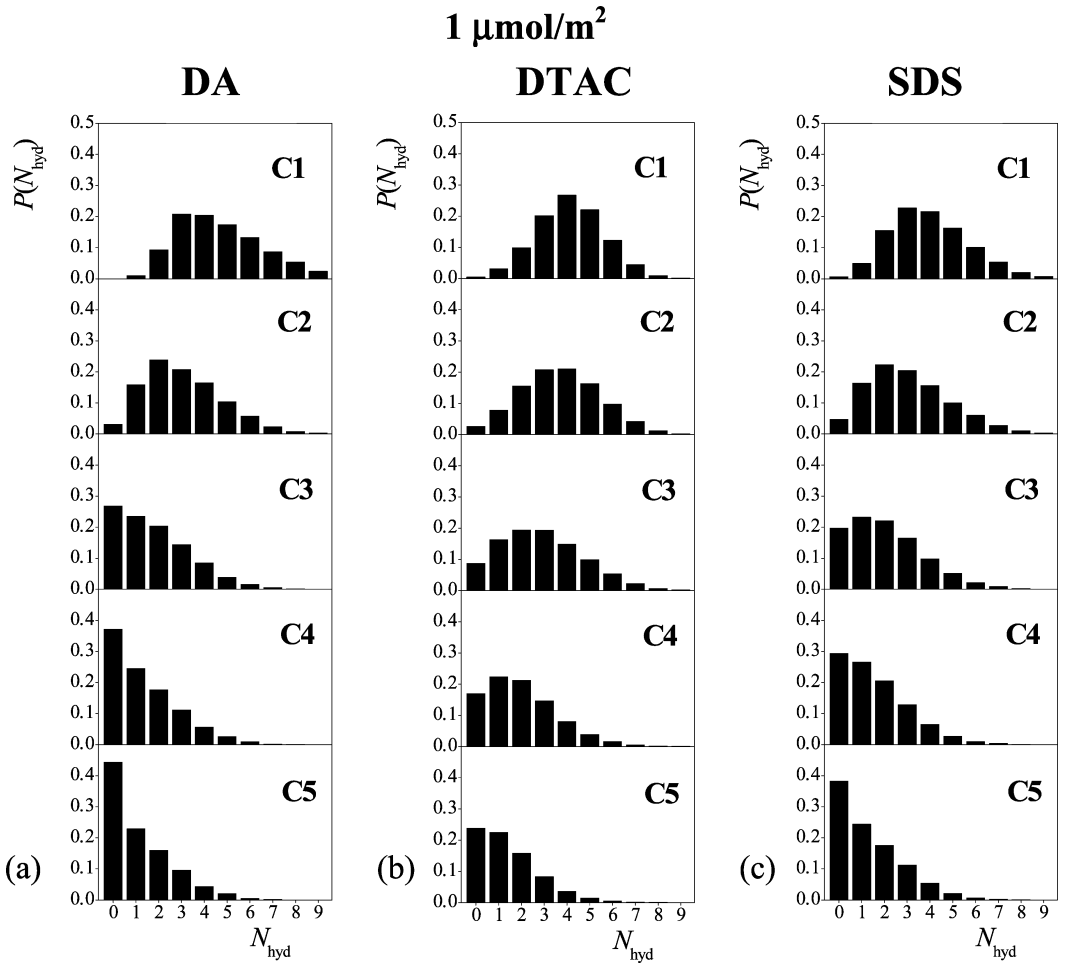

Figure 9. Distribution of the hydration number of the C1 (top panels), C2 (second panels), C3 (third panels), C4 (fourth panels), and C5 (bottom panels) tail carbon atoms of (a) DA, (b) DTAC, and (c) SDS at the surface density of 1 μmol/m^2. Tail carbon atoms are numbered from the headgroup toward the terminal methyl group. (See Figure 1.)

dx.doi.org/10.1021/jp401749r | J. Phys. Chem. B 2013, 117, 8733−8746

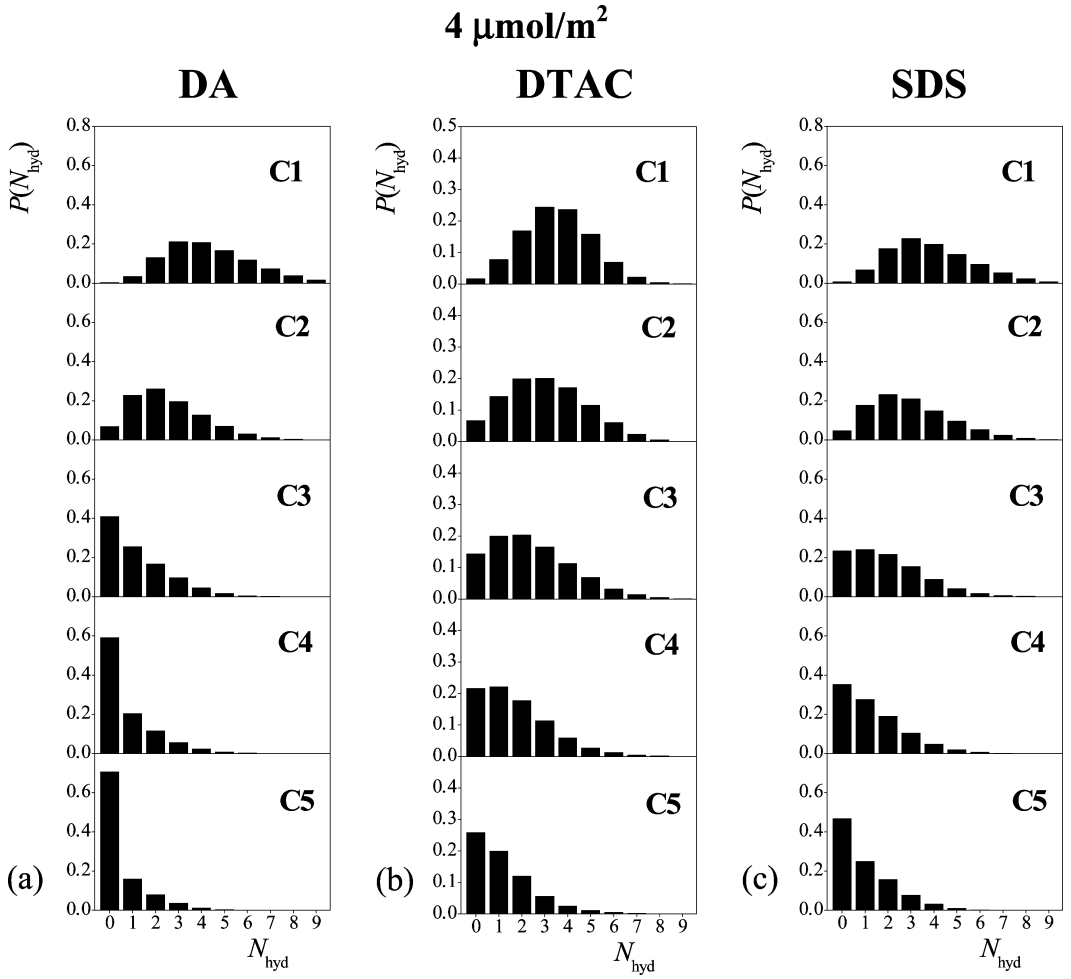

Figure 10. Distribution of the hydration number of the C1 (top panels), C2 (second panels), C3 (third panels), C4 (fourth panels), and C5 (bottom panels) tail carbon atoms of (a) DA, (b) DTAC, and (c) SDS at the surface density of 4 μmol/m^2. Tail carbon atoms are numbered from the headgroup toward the terminal methyl group. (See Figure 1.)

three to four contact water neighbors also occur with noticeable probabilities, even in the systems of 4 μmol/m^2 surface density.

In the case of the unsaturated systems these findings can be interpreted as a consequence of the preferred tilted orientation of the surfactants. However, for saturated systems the non-negligible hydration of even the fifth tail carbon atom suggests that the surfactants are likely to be immersed into the aqueous phase to a certain extent.

To further investigate this problem we have calculated the composition of the subsequent subsurface layers of the aqueous phase in every system up to the point where the vast majority (i.e., at least 95%) of the atoms in the given layer are water oxygens. (Note that hydrogen atoms are excluded from these analyses.) The resulting data are summarized in Tables 1−3 for the alcoholic surfactants, DTAC, and SDS, respectively, and are also shown in Figure 11 for the first seven layers of the two ionic surfactants at 4 μmol/m^2.

As it is seen, there is a clear difference in the behavior of the alcoholic and ionic surfactants in this respect. Thus, in the case of the alcoholic surfactants tail C atoms are typically present in the first and alcoholic oxygens in the second layer of the aqueous phase, while the third layer is almost exclusively formed by water oxygens in all of these systems. Thus, in the case of the 1 and 4 μmol/m^2 alcoholic systems, 15−35% and 60−80% of the first layer, respectively, is built up by tail carbon

Table 1. Composition of the Subsequent Subsurface Layers of the Aqueous Phase in the Systems Containing Alcoholic Surfactants

			percentage of various atoms in the layer		
surfactant	surface density	layer	water O	tail C	headgroup O
PA	1 μmol/m^2	1	81.5	17.2	1.3
		2	94.5	1.8	3.7
		3	99.0	0.5	0.5
	4 μmol/m^2	1	35.9	60.5	3.6
		2	73.8	10.7	15.5
		3	96.8	0.9	2.3
OA	1 μmol/m^2	1	73.6	25.2	1.2
		2	92.7	3.7	3.6
		3	99.5	0	0.5
	4 μmol/m^2	1	27.8	69.5	2.7
		2	69.4	14.9	15.7
		3	95.9	0.9	3.2
DA	1 μmol/m^2	1	65.3	33.9	0.8
		2	88.5	7.8	3.7
		3	98.6	0.5	0.9
	4 μmol/m^2	1	19.2	78.6	2.2
		2	65.0	20.2	15.0
		3	95.0	1.4	3.6

dx.doi.org/10.1021/jp401749r | J. Phys. Chem. B 2013, 117, 8733−8746

Table 2. Composition of the Subsequent Subsurface Layers of the Aqueous Phase in the Systems Containing DTAC

surface density	layer	percentage of various atoms in the layer				
		water O	tail C	headgroup N	headgroup C	Cl^-
1 μmol/m^2	1	70.2	28.5	0	1.0	0.3
	2	76.5	16.5	0	5.7	1.3
	3	86.2	5.6	0.7	6.2	1.3
	4	92.4	1.1	2.6	2.9	1.0
	5	96.8	0.1	1.7	0.8	0.6
4 μmol/m^2	1	28.4	67.2	0	3.0	1.4
	2	35.4	50.3	0	10.9	3.4
	3	48.8	29.5	1.9	14.9	4.9
	4	59.3	15.8	4.6	15.6	4.7
	5	73.7	6.2	5.1	11.9	3.3
	6	85.55	1.8	5.1	5.7	1.9
	7	93.0	1.0	3.1	1.9	1.0
	8	96.5	1.1	1.2	0.6	0.6

Table 3. Composition of the Subsequent Subsurface Layers of the Aqueous Phase in the Systems Containing SDS

surface density	layer	percentage of various atoms in the layer					
		water O	tail C	headgroup S	headgroup −O−	headgroup =O	Na^+
1 μmol/m^2	1	64.4	34.76	0	0	0.9	0
	2	80.87	11.3	0	0	6.9	1.0
	3	90.0	1.8	0	0.6	6.0	1.6
	4	93.1	0.20	0.6	3.1	1.9	1.1
	5	94.5	0	3.1	1.4	0.3	0.7
	6	97.9	0	1.4	0.3	0.0	0.4
4 μmol/m^2	1	16.0	82.9	0	0	1.1	0
	2	41.0	42.1	0	0	13.9	3.0
	3	58.0	14.5	0	0.6	21.1	5.8
	4	68.4	5.4	0.6	6.2	14.6	4.8
	5	75.9	1.4	6.2	7.0	6.7	2.8
	6	84.8	0.3	7.2	3.7	2.4	1.7
	7	93.1	0	3.8	1.6	0.6	0.9
	8	97.3	0	1.6	0.4	0.1	0.6

atoms. This value drops by about a factor of 10, i.e., to 0.5−3.5% in the second layer, where the mole percentage of the alcoholic O atoms is much higher than that in the other layers, being ∼4% at 1 μmol/m^2 and 15−16% at 4 μmol/m^2. Finally, water oxygens give 99% and 95−97% of the third layer at 1 and 4 μmol/m^2, respectively. Considering our definition of the aqueous phase (see Section 2.2), namely, that tail carbon atoms being in direct contact with water are also regarded as part of the aqueous phase, these results are compatible with the classic picture that the polar headgroup is located right at the water surface and the apolar tails are practically not immersed into the aqueous phase.

A completely different picture is seen, however, in the case of the two ionic surfactants considered in this study. Thus, the mole percentage of the tail carbons is still 2−6% in the third layer (at 1 μmol/m^2) and 6−16% in the fourth layer (at 4 μmol/m^2) of these systems. The mole percentage of the first headgroup atoms is the highest in the fourth and in the fifth subsurface layers in the unsaturated and saturated systems, respectively, and headgroup atoms form a nonvanishing fraction (i.e., ∼2%) of even the fifth−sixth (at 1 μmol/m^2) and eighth layers (at 4 μmol/m^2) beneath the water surface. It should further be noted that the fraction of the headgroup atoms is clearly larger in these layers, deeply below the water surface than in the surface layer itself. Thus, contrary to the alcoholic surfactants, these ionic surfactants are indeed immersed several molecular layers deep into the aqueous phase, and this immersion depth is somewhat larger at the surface density of 4 than of 1 μmol/m^2.

Finally, to quantify this immersion depth, we have calculated the distribution of the different surfactant atom types between the subsequent molecular layers of the aqueous phase. The data obtained at the surface densities of 1 and 4 μmol/m^2 are collected in Tables 4 and 5, respectively, and are also shown in Figure 12 for the two ionic surfactants considered. These results confirm our above finding about the different immersion behavior of the alcoholic and ionic surfactants. Thus, no atom of the alcoholic surfactants reaches the fourth subsurface layer of the aqueous phase in any case. The vast majority, i.e., 80−90%, of the tail carbon atoms that are regarded to be part of the aqueous phase are located in the first layer, and not more than 2% of these atoms can reach the third layer. Furthermore, ∼70% of the alcoholic oxygens are located in the second subsurface layer in every case.

Because of the definition we used for the aqueous phase, i.e., that tail carbon atoms having at least one contact water neighbor are also regarded to be part of this phase, a large number of tail carbons should be found in the first layer even if the surfactants are not immersed in water. This is clearly an artifact; in other words, this is the price we have to pay for not missing any of the really immersed tail carbons from the aqueous phase. However, if the hydrocarbon tails are not

dx.doi.org/10.1021/jp401749r | J. Phys. Chem. B 2013, 117, 8733−8746

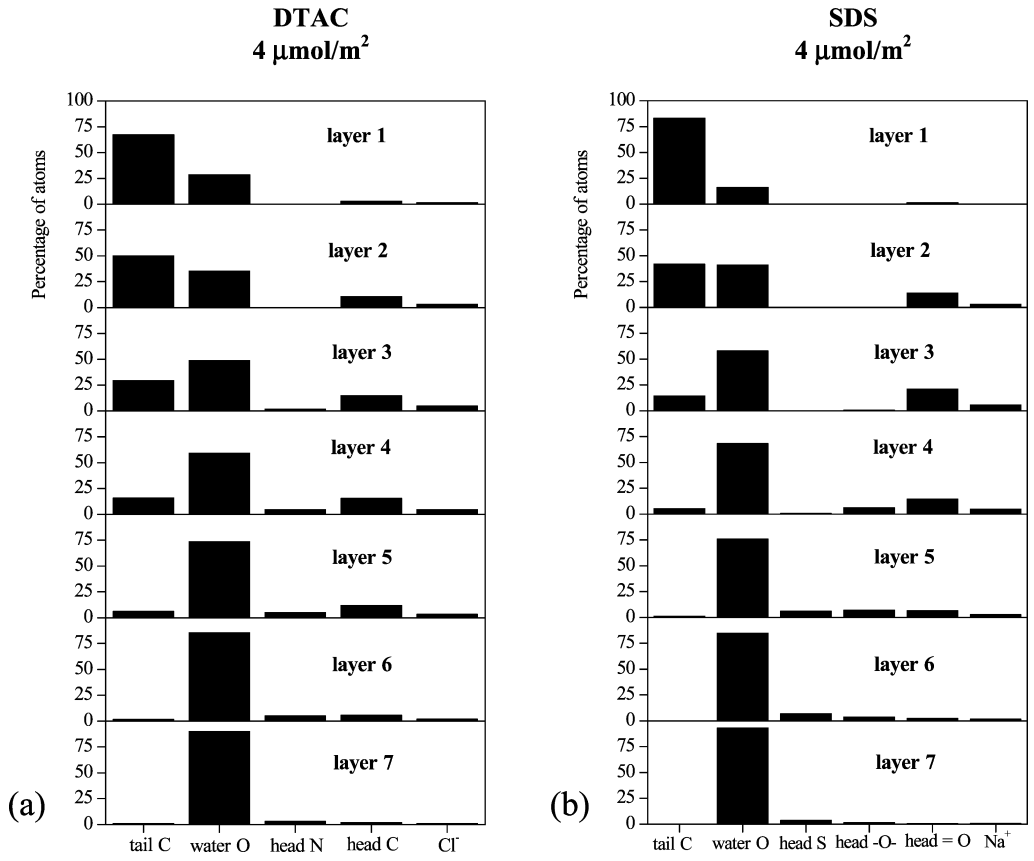

Figure 11. Percentage of the different atom types in the first seven subsurface layers (panels from top to bottom) of the aqueous phase of the systems containing (a) DTAC and (b) SDS at the surface density of 4 μmol/m^2.

Table 4. Distribution of the Different Headgroup Atoms (in Percentage) Between the Subsequent Subsurface Layers of the Aqueous Phase in the Systems Containing Surfactant at the Surface Density of 1 μmol/m^2

		subsurface layer number						
surfactant	atom	1	2	3	4	5	6	7
PA	tail CH_2	89.1	8.7	2.2	0	0	0	0
	O	25.0	66.7	8.3	0	0	0	0
OA	tail CH_2	88.4	11.6	0	0	0	0	0
	O	25.0	66.7	8.3	0	0	0	0
DA	tail CH_2	82.2	16.8	1.0	0	0	0	0
	O	16.7	66.7	16.6	0	0	0	0
DTAC	tail CH_2	58.1	29.9	10.3	1.7	0	0	0
	N	0	0	8.3	50.0	33.4	8.3	0
	head CH_3	5.9	32.3	41.2	17.7	2.9	0	0
	Cl^-	8.3	25.0	25.0	16.7	8.3	8.3	8.3
SDS	tail CH_2	74.3	22.1	3.6	0	0	0	0
	S	0	0	0	8.3	58.3	25.0	8.3
	−O−	0	8.3	58.4	25.0	8.3	0	0
	=O	5.6	41.7	36.1	13.9	2.8	0	0
	Na^+	0	16.7	25	16.7	8.3	8.3	8.3

immersed in the aqueous phase, then far fewer tail carbons should already be found in the second layer than in the first one. This is exactly what is seen for the alcoholic surfactants, for which the number of second layer carbons turned out to be 5−10 times less than in the first layer. It should also be reminded that in the case of saturated layers the composition of the first and second layers is markedly different, with the first containing 60−80% tail carbon, while the latter contain 60−70% water oxygen atoms. (See Table 1.) (In the case of the unsaturated layers the number of tail carbon atoms present in the system is simply not enough to form the major fraction of even a single layer.) All of these findings reveal that alcoholic surfactants do not immerse into the aqueous phase. The tail carbon atoms are, in fact, located above the water, and, despite our definition, they are not part of the aqueous phase, whereas the alcoholic headgroups are predominantly located at the surface of the aqueous phase.

dx.doi.org/10.1021/jp401749r | J. Phys. Chem. B 2013, 117, 8733−8746

Table 5. Distribution of the Different Headgroup Atoms (in Percentage) Between the Subsequent Subsurface Layers of the Aqueous Phase in the Systems Containing Surfactant at the Surface Density of 4 μmol/m^2

		subsurface layer number						
surfactant	atom	1	2	3	4	5	6	7
PA	tail CH_2	83.9	14.9	1.2	0	0	0	0
	O	16.7	72.9	10.4	0	0	0	0
OA	tail CH_2	81.6	17.4	1.0	0	0	0	0
	O	12.5	72.9	14.6	0	0	0	0
DA	tail CH_2	79.3	19.4	1.3	0	0	0	0
	O	10.6	70.2	19.2	0	0	0	0
DTAC	tail CH_2	42.0	27.4	15.9	8.5	3.2	1.0	0.5
	N	0	0	8.3	28.3	25.0	22.9	14.6
	head CH_3	5.6	17.4	22.8	23.6	17.4	9.0	3.5
	Cl^-	8.3	16.7	22.9	20.8	14.6	8.3	4.2
SDS	tail CH_2	58.1	26.9	10.1	3.8	0.9	0.3	0
	S	0	0	0	4.2	31.3	35.4	18.8
	−O−	0	0	4.2	31.3	35.4	18.8	8.3
	=O	1.4	23.6	33.3	24.3	12.5	4.1	0.8
	Na^+	0	14.6	29.2	25.0	14.6	8.3	4.1

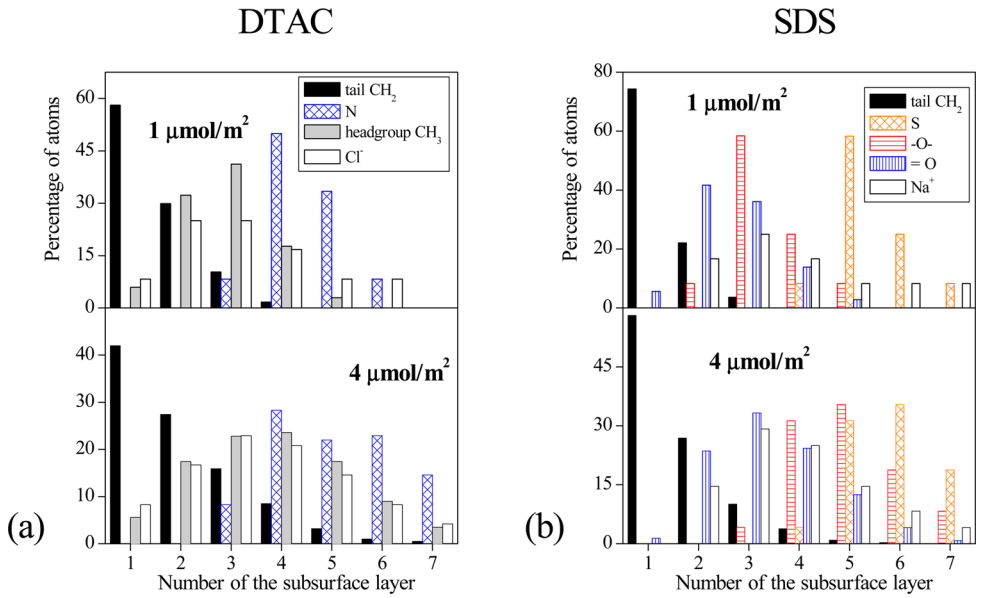

Figure 12. Distribution of various surfactant atom types between the first seven subsurface layers of the aqueous phase of the systems containing (a) DTAC and (b) SDS at the surface densities of 1 μmol/m^2 (top panels) and 4 μmol/m^2 (bottom panels). Data corresponding to the tail C, headgroup N and C (for DTAC) and headgroup S, single-bonded O and double-bonded O (for SDS) atoms are shown by black-filled, blue-squared, gray-filled, orange-squared, red horizontally striped, and blue vertically striped columns, respectively.

The majority of the tail carbon atoms of the two ionic surfactants are also located in the first layer of the aqueous phase. This can again be partially an artifact due to our present definition of the aqueous phase. However, in the case of these surfactants a noticeable fraction of the tail carbons can reach the third−fourth, and in some cases even the fifth subsurface layer. The central N atom of the DTAC and central S atom of the SDS headgroup are typically located in the fourth−sixth subsurface layer, while oxygens of the SDS headgroup can typically be found three to five layers below the surface of the aqueous phase. All of these findings reflect that, contrary to the alcoholic molecules, the ionic DTAC and SDS surfactants are immersed into the aqueous phase, in the depth of several molecular layers of water. This conclusion is not changed even if the aqueous character of the first layer (according to our definition) can be questioned in some cases; the difference in the immersion behavior of the ionic and alcoholic surfactants is clearly revealed by the above analyses.

In understanding the origin of this different immersion behavior of the ionic and alcoholic surfactants, one has to consider the fact that the alcoholic OH groups can fit well to the hydrogen-bonding pattern of the surface water molecules, while the alkyl groups of these alcohols can effectively replace the dangling H atoms[61,62] of the surface water molecules.[48] The ionic headgroups, bearing a net charge, change the orientation of the hydrating water molecules and hence are expected to deteriorate the hydrogen-bonding pattern of the surface water molecules if they are also in the surface layer. Furthermore, contacts of these ionic groups with water molecules are energetically clearly far more preferable than those with tail carbon atoms. Thus, ionic headgroups are immersed several layers deep into the aqueous phase to guarantee full hydration,

dx.doi.org/10.1021/jp401749r | J. Phys. Chem. B 2013, 117, 8733−8746

and this immersion of the headgroup also pulls the first few carbon atoms of the hydrocarbon tail into the aqueous phase.

4. SUMMARY AND CONCLUSIONS

We analyzed in detail, to the best of our knowledge, for the first time, the immersion depth of different ionic and nonionic surfactant molecules into the aqueous phase at the free water surface by computer simulation methods, in terms of subsurface atomistic layers. This kind of analysis is enabled by the use of an intrinsic surface analysis method (in our case, ITIM[43]), which allows one to identify the atoms forming the surface layer of a condensed phase as well as those forming the subsequent layers beneath the surface.

Besides water and headgroup atoms, here we also regarded tail carbon atoms having a contact water neighbor as part of the aqueous phase. (For simplicity, H atoms were omitted from these analyses.) Although this definition also counts several nonimmersed carbon atoms (i.e., the ones being just above the water phase but still in contact with it) as part of the first aqueous layer, our analyses turned to be able to distinguish between nonimmersed and immersed surfactant types and (apart from the uncertainty of the first layer of not clearly aqueous character) also to quantify the immersion depth of the latter type of surfactants. In particular, a clear difference is found in the behavior of the alcoholic and ionic surfactants with respect of their immersion. Thus, alcoholic surfactants behave according to the classical picture; i.e., their headgroups are located in the surface layer of the aqueous phase and the apolar tails above the water surface. This behavior is compatible with the fact that alcoholic oxygens can replace water oxygens in the laterally percolating[63] hydrogen-bonding network of the surface molecules, while the hydrocarbon tails can effectively replace dangling hydrogens[61,62] and hence decrease the surface tension of the system.[48]

Ionic surfactants are immersed several layers deep into the aqueous phase, with tail carbons being present in the third−fourth and headgroup atoms in some cases even in the eighth subsurface layer. This immersion depth is somewhat larger for the saturated than for the unsaturated adsorption layers. The main thermodynamic driving force of this behavior is the energy gain of the ionic headgroups being fully surrounded by water neighbors instead of being in contact with the apolar tails. This immersion of the ionic headgroup pulls then also several carbon atoms of the hydrocarbon tail into the aqueous environment.

It should finally be noted that the observed difference between the behavior of the ionic and nonionic surfactants in this respect correlates well with the experimental observation of Gragson et al., namely, that ionic surfactants enhance the orientational order of the water molecules, while nonionic surfactants have no such effect.[5] Considering that penetration of water molecules into the surfactants (or, equivalently, surfactant penetration into water) is expected to enhance the water orientational ordering (because of the partial loss of the H-bonded neighbors and also the weaker screening of the headgroup charge), our main finding is also supported by some experimental evidence.

■ ASSOCIATED CONTENT

Supporting Information

Intramolecular parameters of the force field used in the simulations. This material is available free of charge via the Internet at http://pubs.acs.org.

■ AUTHOR INFORMATION

Corresponding Author

*E-mail: pali@chem.elte.hu.

Notes

The authors declare no competing financial interest.

■ ACKNOWLEDGMENTS

This project is supported by the Hungarian OTKA Foundation under project no. 104234.

■ REFERENCES

(1) Lu, J. R.; Simister, E. A.; Lee, E. M.; Thomas, R. K.; Rennie, A. R.; Penfold, J. Direct Determination by Neutron Reflection of the Penetration of Water into Surfactant Layers at the Air/Water Interface. *Langmuir* **1992**, *8*, 1837−1844.

(2) Lu, J. R.; Simister, E. A.; Thomas, R. K.; Penfold, J. Structure of an Octadecyltrimethylammonium Bromide Layer at the Air/Water Interface Determined by Neutron Reflection: Systematic Errors in Reflectivity Measurements. *J. Phys. Chem.* **1993**, *97*, 6024−602.

(3) Messmer, M. C.; Conboy, J. C.; Richmond, G. L. Observation of Molecular Ordering at the Liquid-Liquid Interface by Resonant Sum Frequency Generation. *J. Am. Chem. Soc.* **1995**, *117*, 8039−8040.

(4) Conboy, J. C.; Messmer, M. C.; Richmond, G. L. Investigation of Surfactant Conformation and Order at the Liquid−Liquid Interface by Total Internal Reflection Sum-Frequency Vibrational Spectroscopy. *J. Phys. Chem.* **1996**, *100*, 7617−7622.

(5) Gragson, D. E.; McCarty, B. M.; Richmond, G. L. Surfactant/Water Interactions at the Air/Water Interface Probed by Vibrational Sum Frequency Generation. *J. Phys. Chem.* **1996**, *100*, 14272−14275.

(6) Bain, C. D. Studies of adsorption at interfaces by optical techniques: Ellipsometry, second harmonic generation and sum-frequency generation. *Curr. Opin. Colloid Interface Sci.* **1998**, *3*, 287−292.

(7) Li, Z. X.; Dong, C. C.; Thomas, R. K. Neutron Reflectivity Studies of the Surface Excess of Gemini Surfactants at the Air−Water Interface. *Langmuir* **1999**, *15*, 4392−4396.

(8) Stubenrauch, C.; Albouy, P. A.; von Klitzing, R.; Langevin, D. Polymer/Surfactant Complexes at the Water/Air Interface: A Surface Tension and X-ray Reflectivity Study. *Langmuir* **2000**, *16*, 3206−3213.

(9) Lu, J. R.; Thomas, R. K.; Penfold, J. Surfactant Layers at the Air/Water Interface: Structure and Composition. *Adv. Colloid Interface Sci.* **2000**, *84*, 143−304.

(10) Benderskii, A. V.; Eisenthal, K. B. Aqueous Solvation Dynamics at the Anionic Surfactant Air/Water Interface. *J. Phys. Chem. B.* **2001**, *105*, 6698−6703.

(11) Gilányi, T.; Varga, I.; Mészáros, R. Specific Counterion Effect on the Adsorption of Alkali Decyl Sulfate Surfactants at Air/Solution Interface. *Phys. Chem. Chem. Phys.* **2004**, *6*, 4348−4346.

(12) Ma, G.; Allen, H. C. Real-Time Investigation of Lung Surfactant Respreading with Surface Vibrational Spectroscopy. *Langmuir* **2006**, *22*, 11267−11274.

(13) Kirsch, M. J.; D'Auria, R.; Brown, M. A.; Tobias, D. J.; Hemminger, J. C.; Ammann, M.; Starr, D. E.; Bluhm, H. The Effect of an Organic Surfactant on the Liquid-Vapor Interface of an Electrolyte Solution. *J. Phys. Chem. C.* **2007**, *111*, 13497−13509.

(14) Sloutskin, E.; Sapir, Z.; Bain, C. D.; Lei, Q.; Wilkinson, K. M.; Tamam, L.; Deutsch, M.; Ocko, B. M. Wetting, Mixing, and Phase Transitions in Langmuir-Gibbs Films. *Phys. Rev. Lett.* **2007**, *99*, 136102-1−136102-4.

(15) Zhang, Z.; Zheng, D.; Guo, Y.; Wang, H. Water Penetration/Accommodation and Phase Behaviour of the Neutral Langmuir Monolayer at the Air/Water Interface Probed with Sum Frequency Generation Vibrational Spectroscopy (SFG-VS). *Phys. Chem. Chem. Phys.* **2009**, *11*, 991−1002.

(16) de Aguiar, H. B.; Scheu, R.; Jena, K. C.; de Beer, A. G. F.; Roke, S. Comparison of Scattering and Reflection SFG: a Question of Phase-Matching. *Phys. Chem. Chem. Phys.* **2012**, *14*, 6826−6832.

(17) Angus-Smyth, A.; Campbell, R. A.; Bain, C. D. Dynamic Adsorption of Weakly Interacting Polymer/Surfactant Mixtures at the Air/Water Interface. *Langmuir* **2012**, *28*, 12479−12492.
(18) Gong, H.; Xu, G.; Liu, T.; Xu, L.; Zhai, X.; Zhang, J.; Lv, X. Aggregation Behaviors of PEO-PPO-ph-PPO-PEO and PPO-PEO-ph-PEO-PPO at an Air/Water Interface: Experimental Study and Molecular Dynamics Simulation. *Langmuir* **2012**, *28*, 13590−13600.
(19) Böcker, J.; Schlenkirch, M.; Bopp, P.; Brickmann, J. Molecular Dynamics Simulation of a *n*-Hexadecyltrimethylammonium Chloride Monolayer. *J. Phys. Chem.* **1992**, *96*, 9915−9922.
(20) Tarek, M.; Tobias, D. J.; Klein, M. L. Molecular Dynamics Simulation of Tetradecyltrimethylammonium Bromide Monolayers at the Air/Water Interface. *J. Phys. Chem.* **1995**, *99*, 1393−1402.
(21) Schweighofer, K.; Essman, U.; Berkowitz, M. Simulation of Sodium Dodecyl Sulfate at the Water-Vapor and Water-Carbon Tetrachloride Interfaces at Low Surface Coverage. *J. Phys. Chem. B* **1997**, *101*, 3793−3799.
(22) Schweighofer, K.; Essman, U.; Berkowitz, M. Structure and Dynamics of Water in the Presence of Charged Surfactant Monolayers at the Water-CCl_4 Interface. A Molecular Dynamics Study. *J. Phys. Chem. B* **1997**, *101*, 10775−10780.
(23) Schweighofer, K.; Benjamin, I. Transfer of a Tetramethylammonium Ion across the Water−Nitrobenzene Interface: Potential of Mean Force and Nonequilibrium Dynamics. *J. Phys. Chem. A* **1999**, *103*, 10274−10279.
(24) Domínguez, H.; Berkowitz, M. Computer Simulations of Sodium Dodecyl Sulfate at Liquid/Liquid and Liquid/Vapor Interfaces. *J. Phys. Chem. B* **2000**, *104*, 5302−5308.
(25) Domínguez, H. Computer Simulations of Surfactant Mixtures at the Liquid/Liquid Interface. *J. Phys. Chem. B* **2002**, *106*, 5915−5924.
(26) Jedlovszky, P.; Varga, I.; Gilányi, T. Adsorption of 1-Octanol at the Free Water Surface As Studied by Monte Carlo Simulation. *J. Chem. Phys.* **2004**, *120*, 11839−11851.
(27) Domínguez, H. Computer Simulation Studies of Surfactant Monolayer Mixtures at the Water/Oil Interface: Charge Distribution Effects. *J. Colloid Interface Sci.* **2004**, *274*, 665−672.
(28) Paszternák, A.; Kiss, É.; Jedlovszky, P. Structure of the Nonionic Surfactant Triethoxy Monooctylether C_8E_3 Adsorbed at the Free Water Surface, As Seen from Surface Tension Measurements and Monte Carlo Simulations. *J. Chem. Phys.* **2005**, *122*, 124704.
(29) Domínguez, H.; Rivera, M. Mixtures of Sodium Dodecyl Sulfate/Dodecanol at the Air/Water Interface by Computer Simulations. *Langmuir* **2005**, *21*, 7257−7262.
(30) Rodriguez, J.; Clavero, E.; Laria, D. Computer Simulations of Catanionic Surfactants Adsorbed at Air/Water Interfaces. *J. Phys. Chem. B.* **2005**, *109*, 24427−24433.
(31) Chanda, J.; Bandyopadhyay, S. Molecular Dynamics Study of Surfactant Monolayers Adsorbed at the Oil/Water and Air/Water Interfaces. *J. Phys. Chem. B.* **2006**, *110*, 23482−23488.
(32) Hantal, Gy.; Pártay, L. B.; Varga, I.; Jedlovszky, P.; Gilányi, T. Counterion and Surface Density Dependence of the Adsorption Layer of Ionic Surfactants at the Vapor-Aqueous Solution Interface: A Computer Simulation Study. *J. Phys. Chem. B.* **2007**, *111*, 1769−1774.
(33) Darvas, M.; Gilányi, T.; Jedlovszky, P. Adsorption of Poly(ethylene oxide) at the Free Water Surface. A Computer Simulation Study. *J. Phys. Chem. B.* **2010**, *114*, 10995−11001.
(34) Martínez, H.; Chacón, E.; Tarazona, P.; Bresme, F. The Intrinsic Interfacial Structure of Ionic Surfactant Monolayers at Water-Oil and Water-Vapour Interfaces. *Proc. R. Soc. A* **2011**, *467*, 1939−1958.
(35) Bresme, F.; Chacón, E.; Martínez, H.; Tarazona, P. Adhesive Transitions in Newton Black Films: A Computer Simulation Study. *J. Chem. Phys.* **2011**, *134*, 214701-1−214701-12.
(36) Darvas, M.; Gilányi, T.; Jedlovszky, P. Competitive Adsorption of Surfactants and Polymers at the Free Water Surface. A Computer Simulation Study of the Sodium Dodecyl Sulfate-Poly(ethylene oxide) System. *J. Phys. Chem. B.* **2011**, *115*, 933−944.
(37) Pang, J.; Wang, Y.; Xu, G.; Han, T. Molecular Dynamics Simulation of SDS, DTAB, and $C_{12}E_8$ Monolayers Adsorbed at the Air/Water Surface in the Presence of DSEP. *J. Phys. Chem. B.* **2011**, *115*, 2518−2526.
(38) Rideg, N. A.; Darvas, M.; Varga, I.; Jedlovszky, P. Lateral Dynamics of Surfactants at the Free Water Surface. A Computer Simulation Study. *Langmuir* **2012**, *28*, 14944−14953.
(39) Vacha, R.; Roke, S. Sodium Dodecyl Sulfate at Water−Hydrophobic Interfaces: A Simulation Study. *J. Phys. Chem. B.* **2012**, *116*, 11936−11942.
(40) Chacón, E.; Tarazona, P. Intrinsic Profiles beyond the Capillary Wave Theory: A Monte Carlo Study. *Phys. Rev. Lett.* **2003**, *91*, 166103-1−166103-4.
(41) Chowdhary, J.; Ladanyi, B. M. Water-Hydrocarbon Interfaces: Effect of Hydrocarbon Branching on Interfacial Structure. *J. Phys. Chem. B.* **2006**, *110*, 15442−15453.
(42) Jorge, M.; Cordeiro, M. N. D. S. Intrinsic Structure and Dynamics of the Water/Nitrobenzene Interface. *J. Phys. Chem. C.* **2007**, *111*, 17612−17626.
(43) Pártay, L. B.; Hantal, Gy.; Jedlovszky, P.; Vincze, Á.; Horvai, G. A New Method for Determining the Interfacial Molecules and Characterizing the Surface Roughness in Computer Simulations. Application to the Liquid−Vapor Interface of Water. *J. Comput. Chem.* **2008**, *29*, 945−956.
(44) Wilard, A. P.; Chandler, D. Instantaneous Liquid Interfaces. *J. Phys. Chem. B.* **2010**, *114*, 1954−1958.
(45) Jorge, M.; Jedlovszky, P.; Cordeiro, M. N. D. S. A Critical Assessment of Methods for the Intrinsic Analysis of Liquid Interfaces. 1. Surface Site Distributions. *J. Phys. Chem. C.* **2010**, *114*, 11169−11179.
(46) Sega, M.; Kantorovich, S.; Jedlovszky, P.; Jorge, M. The Generalized Identification of Truly Interfacial Molecules (ITIM) Algorithm for Nonplanar Interfaces. *J. Chem. Phys.* **2013**, *138*, 044110-1−044110-10.
(47) Hantal, Gy.; Darvas, M.; Pártay, L. B.; Horvai, G.; Jedlovszky, P. Molecular Level Properties of the Free Water Surface and Different Organic Liquid/Water Interfaces, as Seen from ITIM Analysis of Computer Simulation Results. *J. Phys.: Condens. Matter* **2010**, *22*, 284112-1−1284112-14.
(48) Pártay, L. B.; Jedlovszky, P.; Vincze, Á.; Horvai, G. Properties of Free Surface of Water-Methanol Mixtures. Analysis of the Truly Interfacial Molecular Layer in Computer Simulation. *J. Phys. Chem. B.* **2008**, *112*, 5428−5438.
(49) Pártay, L. B.; Jedlovszky, P.; Horvai, G. Structure of the Liquid-Vapor Interface of Water-Acetonitrile Mixtures as Seen from Molecular Dynamics Simulations and Identification of Truly Interfacial Molecules Analysis. *J. Phys. Chem. C.* **2009**, *113*, 18173−18183.
(50) Pojják, K.; Darvas, M.; Horvai, G.; Jedlovszky, P. Properties of the Liquid-Vapor Interface of Water-Dimethyl Sulfoxide Mixtures. A Molecular Dynamics Simulation and ITIM Analysis Study. *J. Phys. Chem. C.* **2010**, *114*, 12207−12220.
(51) Pártay, L. B.; Horvai, G.; Jedlovszky, P. Temperature and Pressure Dependence of the Properties of the Liquid-Liquid Interface. A Computer Simulation and Identification of the Truly Interfacial Molecules Investigation of the Water-Benzene System. *J. Phys. Chem. C.* **2010**, *114*, 21681−21693.
(52) Schuler, L. D.; Daura, X.; van Gunsteren, W. F. An Improved GROMOS96 Force Field for Aliphatic Hydrocarbons in the Condensed Phase. *J. Comput. Chem.* **2001**, *22*, 1205−1218.
(53) van Gunsteren, W. F.; Billeter, S. R.; Eising, A. A.; Hünenberger, P. H.; Krüger, P.; Mark, A. E.; Scott, W. R. P.; Tironi, I. G. *Biomolecular Simulation: The GROMOS96 Manual and User Guide*; vdf Hochschulverlag A.G. an der ETH Zürich and BIOMOS b.v.: Zürich, Groningen, 1996.
(54) Hess, B.; Bekker, H.; Berendsen, H. J. C.; Fraaije, J. G. E. M. LINCS: A Linear Constraint Solver for Molecular Simulations. *J. Comput. Chem.* **1997**, *18*, 1463−1462.
(55) Ryckaert, J. P.; Bellemans, A. Molecular Dynamics of Liquid Alkanes. *Faraday Discuss. Chem. Soc.* **1978**, *66*, 95−106.
(56) Berendsen, H. J. C.; Postma, J. P. M.; van Gunsteren, W. F.; Hermans, J. Interaction Models for Water in Relation to Protein

Hydration. In *Intermolecular Forces*; Pullman, B., Ed.; Reidel: Dordrecht, The Netherlands, 1981; pp 331−342.
(57) Miyamoto, S.; Kollman, P. A. Settle: An Analytical Version of the SHAKE and RATTLE Algorithm for Rigid Water Models. *J. Comput. Chem.* **1992**, *13*, 952−962.
(58) Essman, U.; Perera, L.; Berkowitz, M. L.; Darden, T.; Lee, H.; Pedersen, L. G. a Smooth Particle Mesh Ewald Method. *J. Chem. Phys.* **1995**, *103*, 8577−8594.
(59) Lindahl, E.; Hess, B.; van der Spoel, D. GROMACS 3.0: a Package for Molecular Simulation and Trajectory Analysis. *J. Mol. Model.* **2001**, *7*, 306−317.
(60) Berendsen, H. J. C.; Postma, J. P. M.; DiNola, A.; Haak, J. R. Molecular Dynamics with Coupling to an External Bath. *J. Chem. Phys.* **1984**, *81*, 3684−3691.
(61) Brown, M. G.; Raymond, E. A.; Allen, H. C.; Scatena, L. F.; Richmond, G. L. The Analysis of Interference Effects in the Sum Frequency Spectra of Water Interfaces. *J. Phys. Chem. A.* **2000**, *104*, 10220−10226.
(62) Scatena, L. F.; Brown, M. G.; Richmond, G. L. Water at Hydrophobic Surfaces: Weak Hydrogen Bonding and Strong Orientation Effects. *Science* **2001**, *292*, 908−912.
(63) Darvas, M.; Horvai, G.; Jedlovszky, P. Temperature Dependence of the Lateral Hydrogen Bonded Clusters of Molecules at the Free Water Surface. *J. Mol. Liq.* **2012**, *176*, 33−38.